Experimental Procedure to Optimize Out-Of-Band Terminations for Highly Linear and Power Efficient Bipolar Class-AB RF Amplifiers

M. Spirito[1], M. P. van der Heijden[2], M. Pelk[1], L. C. N. de Vreede[1],
P.J. Zampardi[3], L.E. Larson[4] and J. N. Burghartz[1]

[1]HiTeC Laboratory, Delft University of Technology, Mekelweg 4, 2628 CD Delft, The Netherlands
[2]Philips Research Laboratories, Prof. Holstlaan 4, 5656 AA Eindhoven, The Netherlands
[3]Skyworks Solutions, Inc., Newbury Park, CA 91320 USA
[4]University of California at San Diego, La Jolla, CA 92093 USA

Abstract — **An optimization procedure based on load-pull measurements to obtain both highly-linear and highly-efficient class-AB operation is presented. This procedure can be applied without any foregoing device characterization; therefore it is an excellent method to compare the linearity performance of different bipolar technologies. The presented approach provides the optimum out-of-band terminations and quiescent current yielding IM3 improvement of more than 15 dBc at 3 dB back-off compared to traditional design techniques. Optimum power-added efficiency is achieved at the same time.**

Index Terms — **Load-pull, linearity, out-of-band termination.**

I. Introduction

Class-AB or inverse-class AB amplifier operation is preferred for power amplifiers (PA's) in linear wireless communication systems, since it offers a workable trade-off between linearity and efficiency. When considering pure class-AB amplifier operation, it is customary to cancel the harmonics at the output of the active device to achieve maximum collector efficiency, ideally 78.5% for pure class B [1]. When considering the input matching conditions of the active device, it has been shown that at low power levels (large power back-off conditions) the use of proper out-of-band terminations at baseband and second harmonic frequencies can yield dramatic improvements in linearity without compromising gain or DC power consumption [2,3,4]. These out-of-band termination techniques applied at the input of a bipolar device are based on the cancellation of the 3rd-order intermodulation (IM3) products. This is achieved by compensating the IM3 products resulting from the 3rd-order nonlinearities, by the 3rd-order (IM3) products which result from secondary mixing of the even-order components with the fundamental over the nonlinear base-emitter junction. Only by proper selection of the input out-of-band terminations at the baseband (BB) and the second harmonic it is possible to control this secondary mixing process so that perfect IM3 cancellation can be achieved. This has successfully been demonstrated for various low power circuits such as LNA's [2], [3], mixers [4] and a differential driver stage [5]. Recently, the selection of the optimum quiescent current and proper out-of-band terminations was demonstrated theoretically also at higher power levels [6]. An extended Volterra series analysis supported by circuit simulations was used for that purpose [7]. A shortcoming of that approach was, however, that a complete device characterization and model extraction were required prior to the linearity characterization.

In this paper we present an extended experimental procedure that facilitates linearity optimization on devices without any previous transistor measurement and modeling. Furthermore, the PAE improvements, close to compression, are greatly enhanced compared to the prior work. In Section II, we discuss the in-house developed active harmonic load-pull system that facilitates an accurate control of the base-band impedance. In Section III we utilize this feature to provide a straightforward experimental linearity optimization procedure for BJT devices. First the optimum quiescent current, base-band and 2nd harmonic ohmic impedance, are found. These are characteristic for a given bipolar device and provide the highest linearity over a large bandwidth in back-off conditions. Then, while maintaining the high linearity (Sections IV and V), the sweet spot is shifted towards higher power levels. This is done by changing the quiescent current and the 2nd harmonic termination in a pre-described way. As last point, a relation that links the optimum linearity quiescent current and BB source impedance, is used to reduce the static power dissipation and improve the PAE of the device, not affecting the achieved linearity.

II. Harmonic Load-Pull System for PA Optimization

The measurement system shown in Fig. 1 facilitates

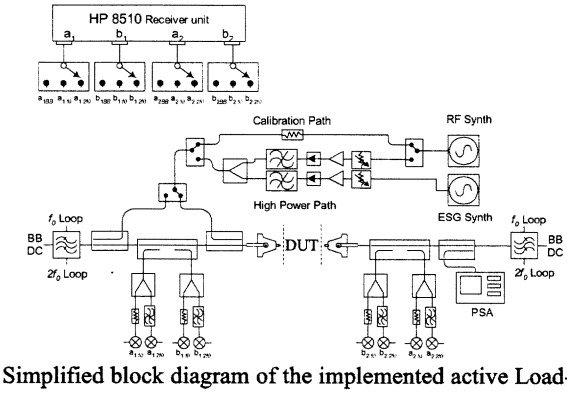

Fig.1. Simplified block diagram of the implemented active Load-Pull system.

independent control of the fundamental (Zf_0), base-band (Zf_{BB}) and second-order (Zf_{2nd}) impedances at the input and output during load-pull measurements [6]. In order to perform a measurement-based out-of-band optimization of power amplifier linearity, several aspects of the measurement setup have to be addressed:

1) The load-pull implementation needs to be active, to compensate for the losses of the setup and facilitate effective conditions for canceling the harmonics.
2) The electrical delay of the system should be kept small, in order to provide realistic matching condition for wideband modulated signals (e.g. CDMA).
3) The base-band impedance must be purely real and accurately reproducible to avoid asymmetries in intermodulation components [7, 8].

These points were all addressed by the new load-pull system implementation. In comparison to [6], the system employs more compact active loops and a new diplexer board, providing >30dB isolation between f_0 and $2{\cdot}f_0$ and low reflection coefficients to the DUT outside the frequency band of the active terminations.

III. Low Power Linearity Optimization

A GaAs HBT from Skyworks with a f_T=40 GHz was used to demonstrate the procedure. The emitter finger dimensions were 22 x 2.2 μm^2, and the device had two emitter, three base, and two collector fingers. After a conventional single-tone load-pull analysis, which was performed to identify the optimum load condition for maximum PAE (measured one-tone peak PAE=60%) with $Z_{2nd\ output}$=0 and $Z_{2nd\ input}$=50 Ω, the system is calibrated for a two-tone signal with Δf=0.5 MHz. At low input power levels, the third-order distortion was mainly generated by the exponential nonlinearities: g_m, g_{be} and the diffusion capacitance (C_d). The third-order distortion contributions of these elements could completely be cancelled, independent of center frequency and tone-spacing [3], provided, that the following requirements on source impedance and bias current are satisfied:

$$Z_{S,BB} = Z_{S,2nd} = \frac{\beta_F}{2g_m}$$
$$C_{jE} = 2\tau_F g_m \qquad (1)$$
$$g_m = \frac{I_c}{V_T}$$

Note, that these requirements fix the optimum quiescent bias current (I_{cq}) for a given bipolar technology at low signal power, namely:

$$I_{cq,opt} = V_T \frac{C_{jE}}{2\tau_F} \qquad (2)$$

Moreover, it was demonstrated in [7] that this unique combination of I_{cq} and purely ohmic [3] base-band source impedances minimizes the asymmetry in the IM3 side-bands. To experimentally find this optimum condition, IM3 versus I_{cq} measurements were performed, while varying the $Z_{S,BB}$=$Z_{S,2nd}$ at a low input power (e.g. -28 dBm tone power). Plotting the maximum upper and lower OIP3 band (achieved in each I_{cq} sweep) as function of $Z_{S,BB}$=$Z_{S,2nd}$ we could find the point of perfect symmetry (Fig. 2).

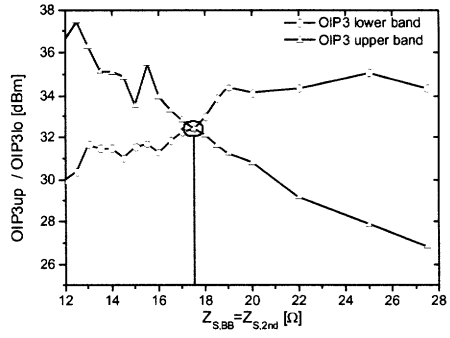

Fig. 2. Measured maximum OIP3 levels for upper and lower IM3 components versus resistive $Z_{S,BB}$ =$Z_{S,2nd}$ from swept I_{cq} conditions (f_0=2.14 GHz, Δf=0.5 MHz).

Note, that this point also provides the optimum linear wide-band behavior. As predicted in [7] this range was significantly wider than 100 MHz. The optimum I_{cq} to bias the device could clearly be identified by plotting the upper and lower OIP3 band versus I_{cq} (Fig. 3) for the impedance value, at which no asymmetry appears ($Z_{S,BB}$=$Z_{S,2nd}$ =17.5 Ohm from Fig. 2). The optimization was performed more than 10dB in back-off, so that the optimum OIP3 levels achieved here are only valid for low signal power levels. In the next sections we will focus on the transfer of the corresponding IM3 cancellation conditions to higher power levels in order to optimize the device linearity closer to the compression point.

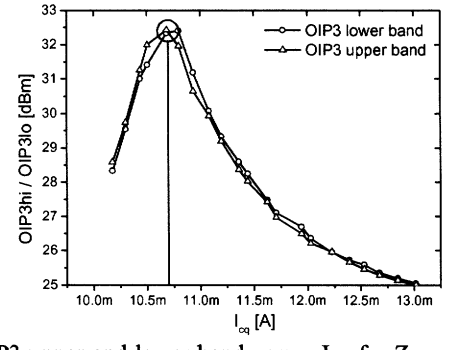

Fig. 3. OIP3 upper and lower band versus I_{cq}, for $Z_{S,BB}$=$Z_{S,2nd}$ =17.5 Ohm and Pin=-28 dBm.

IV. High Power Linearity Optimization

A. Linearity Optimization Theory

The contributions of higher-order nonlinearities cannot be neglected at high power levels. At least a fifth-order Volterra series analysis has therefore to be conducted to allow for valid conclusions about the behavior of the exponential nonlinearities near compression [7]. For this purpose we use the strongly simplified device model shown in Fig. 4. The IM3 components of the nonlinear transfer function can be expressed by [7]:

$$i_{C,IM3} = \frac{3}{4} H_{3,IM3} V_{in}^3 + \frac{25}{8} H_{5,IM3} V_{in}^5 \qquad (3)$$

where $H_{3,IM3}$ and $H_{5,IM3}$ are the 3rd and 5th-order nonlinear transfer functions, respectively. They relate the input voltage magnitude to the third-order distortion generated by the exponential collector current. Fig. 5 (a) shows the simulated $H_{3,IM3}$, $H_{5,IM3}$ when the low-power condition in (1) is met. The optimum $I_{cq,opt}$ for low-power (wide-band) IM3 cancellation is indicated in that plot.

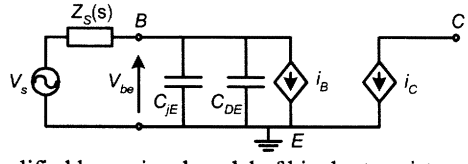

Fig. 4. Simplified large signal model of bipolar transistor.

When an amplifier is biased at exactly this optimum current, the IM3 current only has a 5th-order dependence on the input voltage, because H_3 is zero and H_5 is non-zero. Consequently, if we leave the out-of-band impedances unchanged (17.5 Ohm in this particular case) and only increase I_{cq}, there are V_{in} values, for which (3) becomes zero (since H_3 and H_5 are opposite in sign) and cancellation can occur. This allows for the creation of a "sweet-spot" in the IM3-current at higher input power (V_{in}), degrading the linearity at small signal levels but improving the linearity of the device close to compression. Note, that for bias points below the optimum $I_{cq,opt}$, no cancellation can occur, since *H3* dominates in that region.

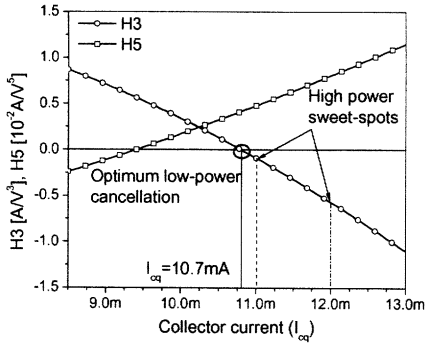

(a)

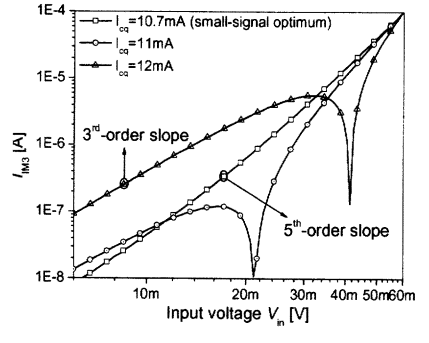

(b)

Fig. 5 (a) Third and fifth-order nonlinear transfer function (H3 and H5) as function of collector current I_{cq}; (b) IM3 current as function of input voltage for different quiescent collector currents.

B. Verification of Linearity Improvement at High Powers

With use of these results, we can experimentally determine the optimum I_{cq} for IM3 cancellation at high power levels. To determine these optimum bias current values, the input power is swept for various I_{cq} values (higher than $I_{cq,opt}$). The input out-of-band terminations are fixed at the values found in the low-power optimization ($Z_{S,BB}$=$Z_{S,2nd}$=17.5 Ohm); this is required to maintain the broad bandwidth of the cancellation. Fig. 6 shows the measured IM3 "sweet spots" at different back-off (BO) power levels. As predicted by theory, the shift in the IM3 cancellation condition near compression is indeed achieved, though for higher I_{cq} values.

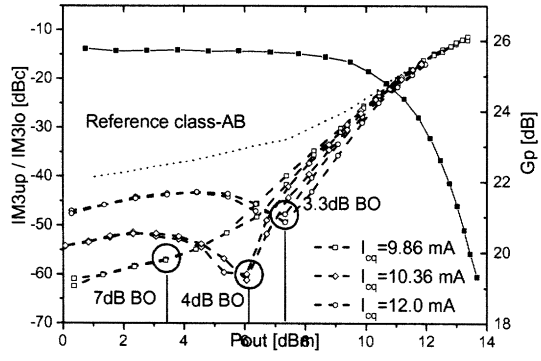

Fig. 6. Measured IM3 (upper and lower band) and Gp versus output power, for three different quiescent current values, with $Z_{S,BB}$= $Z_{S,2nd}$=17.5 Ohm and reference class-AB case.

The reference class-AB curve in Fig. 6 refers to the typical bias case, for which both source and load 2nd and baseband components are shorted ($Z_{S,BB}$=$Z_{S,2nd}$ =0). Note the dramatic improvement in linearity versus power, when using the proposed method (Fig. 6).

V. PAE Optimization

The linearity optimization for the different output power back-off levels has the advantage of maintaining the wideband performance of this solution [7]; this has been shown in Section IV. The trade-off for shifting the IM3 "sweet spot" to a higher power level by increasing I_{cq}, however, is a lower PAE (at the same BO level) than achievable with optimization for efficiency only. To recover this efficiency, we need to reduce the I_{cq} (and thus the g_m) without compromising the optimized linearity. According to (1), the product of $R_{S,BB}$ and g_m must remain constant. Lowering the g_m, however, results in an increased $R_{S,BB}$. That means, that condition (2) is violated, since the depletion capacitance (C_{je}) is fixed for a given device size. The missing imaginary part, required to reestablish the validity of (2), must therefore be provided by a complex 2nd harmonic (2ω) source termination [7], which now will also shift to a higher impedance value (Fig. 7). This results in a diffusion capacitance that is no longer fully "self-compensated" by the base-emitter depletion capacitance. It was theoretically shown in [7] that the cancellation bandwidth is reduced by the presence of base-resistance and the frequency dependence of practical 2nd harmonic terminations. It can be shown for practical implementations, that the higher the Q required for the 2nd harmonic termination, the more narrowband the IM3 cancellation condition will be.

A. Experimental Results

In our experiment we reduced I_{cq} from the nominal value of 12 mA (Case 1) to 7 mA (Case 2) and 6.2 mA (Case 3) and increased similarly $Z_{S,BB}$ to ~26 and ~29 Ohm. The optimum $Z_{S,2nd}$ was found in both cases through a source-pull analysis, leading to complex (inductive) values. Fig. 7 shows the shift in base-band and 2nd harmonic impedance with reduction of current. By moving from Case 1 to Case 3, the PAE is increased while the cancellation bandwidth is reduced due to the higher Q of the 2nd harmonic input termination. Note, that in all three cases the fundamental loading conditions and output out-of-band terminations were kept constant. The measured linearity yielded comparable IM3 upper/lower values in the sweet spot for all three cases, as shown in Fig 8.

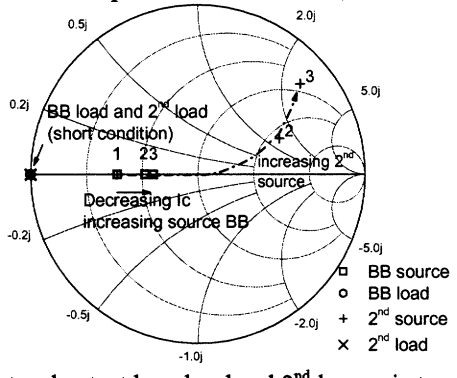

Fig. 7. Input and output base-band and 2nd harmonic termination for the three cases considered for the PAE optimization.

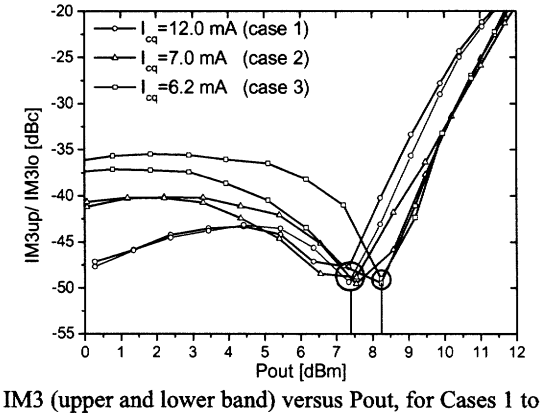

Fig. 8. IM3 (upper and lower band) versus Pout, for Cases 1 to 3.

Fig. 8 also shows that the sweet spot moves to higher power levels for Case 3. This, in conjunction with the reduction in I_{cq}, leads to a higher efficiency for linear device operation, as can be seen from Fig. 9. In this plot the various solutions using pure ohmic out-of-band terminations ($Z_{S,BB}$=$Z_{S,2nd}$=17.5 Ω; see previous section) and the combination of real base-band ($Z_{S,BB}$=17.5 Ω) combined with a complex 2nd-harmonic impedance (this section) are shown, thus confirming the higher efficiency of the latter technique. Even though the IM3 levels now tend to rise at lower power levels than the IM3 sweet spot, this does not appear to affect the linearity

TABLE II
SUMMARY OF PAE OPTIMIZATION

	Case 1	Case 2	Case 3
I_{cq}	12.0 mA	7.0 mA	6.2 mA
OIP3 hi/lo	32.1 dBm	32.1 dBm	33.4dBm
IM3 hi/lo	-48.5 dBc	-49 dBc	-49.5 dBc
Gp	26.1 dB	25.3 dB	25.3 dB
PAE_{CDMA}	21%	29%	31.5%

performance in terms of ACPR when using a realistic modulated signal like IS-95 CDMA. By allowing a maximum ACPR level of -45dBc, we achieved the PAE performance improvements reported in Table II (PAE_{CDMA}).

VII. CONCLUSION

In this paper we have presented an experimental procedure to optimize device linearity at various back-off power levels. Both theory and experimental results show, that also for the wideband cancellation solutions, the I_{cq} can be used to shift the sweet-spot to high power levels. When trading off IM3 cancellation bandwidth, it is also possible to further improve the PAE of the device by using a complex 2nd harmonic input termination.

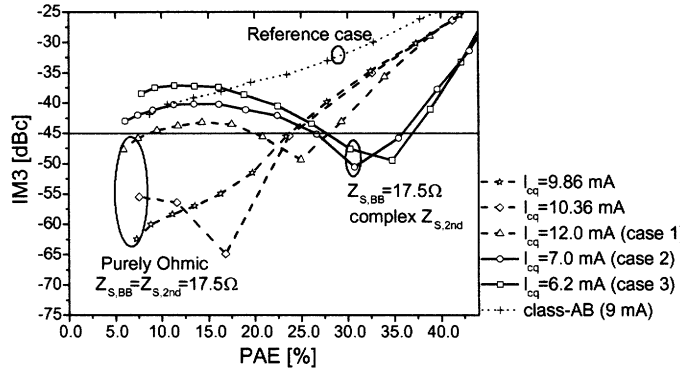

Fig. 9. IM3 versus PAE for the various biasing cases, and the reference class-AB case.

ACKNOWLEDGEMENT

The authors would like to thank A. Akhnoukh of the HiTeC laboratory, Infineon Technologies AG, Skyworks Solutions Inc., Philips Semiconductors, R. Tuijtelaars at BSW, and Maury Microwave, for supporting this project.

REFERENCES

[1] S. C. Cripps, Norwood, MA: Artech House, 2002.
[2] V. Aparin et al. *in 1999 IEEE MTT-S*, pp. 977-980.
[3] M. P. van der Heijden et al. *IEEE JSSC.* Sept. 2002, pp. 1176-83.
[4] S. Liwei, et al. *IEEE MTT,* Nov. 2003, pp.2211 – 2220.
[5] M. P.van der Heijden et.al, *in 2003 IEEE MTT-S*, pp. 235-238.
[6] M. Spirito et al. *in 2004 IEEE MTT-S*, pp. 1215-1218.
[7] M. P.van der Heijden et.al., *BCTM 2004*, pp. 44-4
[8] N. B. Carvalho et al. *in 2000 IEEE MTT-S*, pp. 11-16.